

# A Preliminary Approach for the Segmentation of Mitral Valve Regurgitation Jet in Doppler Ecocardiography Images

Eva Costa<sup>1</sup>, Nelson Martins<sup>1,2</sup>, Malik Saad Sultan<sup>2,3</sup>, Diana Veiga<sup>1</sup>, Manuel João Ferreira<sup>1,4</sup>, Sandra Mattos<sup>5</sup> and Miguel Coimbra<sup>2,3</sup>

<sup>1</sup>*Enemeter, Sistemas de Medição, Lda, Braga, Portugal*

<sup>2</sup>*Faculdade de Ciências, Universidade do Porto, Portugal*

<sup>3</sup>*Instituto de Telecomunicações, Porto, Portugal*

<sup>4</sup>*Centro Algoritmi, University of Minho, Guimarães, Portugal*

<sup>5</sup>*Círculo do Coração de Pernambuco, Recife PE, Brazil*

**Keywords:** Mitral Regurgitation, Echocardiography, Segmentation, Doppler, Heart, Medical Image Processing.

**Abstract:** Rheumatic Fever and Rheumatic Heart Disease remain a major burden among children in developing countries. Echocardiography with colour flow Doppler is key to early diagnosis. However, the technique requires time and experienced operators, which are scarce resources in the affected areas. Automatic segmentation of colour Doppler regurgitation jets could, potentially, reduce the cost of screening, and spread diagnostic accessibility for a larger number of patients. Ultrasound processing is very challenging due to speckle noise and similarity of representation of all kinds of tissue. Region-based active contours are suitable tools for the segmentation in cases of intensity heterogeneities, which makes them interesting algorithms for left atrium segmentation. HSV colour space describes colour in terms of hues and saturation, which may facilitate the translation of medical interpretation of the Doppler pseudo-colour into mathematical expression for colour segmentation. A total of 979 frames from 20 sequences were manually annotated and used to validate the proposed pipeline. Overall, the results for colour pattern segmentation are promising (sensitivity=0.91 false detection rate=0.10), but further developments are required for the atrium segmentation (sensitivity=0.80, false detection rate=0.28).

## 1 INTRODUCTION

Rheumatic Heart Disease (RHD) is the chronic, longterm sequel of repeated untreated Acute Rheumatic Fever (ARF) episodes (E. Marijon, 2009). ARF results from an autoimmune hyper response to untreated streptococcal infections of the pharynx. Most of the patients endure active heart inflammation (carditis) for several months, with the vast majority having valvulitis on the left side of the heart. The most affected structure is the mitral valve complex, which is essential to ensure the unidirectional systemic blood flow from the left atrium to the left ventricle. Structural changes, such as thickening or retraction of the valve and its valvar apparatus, are often found in RHD patients. This may cause severe strain to the heart leading to abnormal function with prolapse, stenosis and/or regurgitation. The major burden of ARF is found among children (5-16 years old) from low to middle income countries and indigenous populations, and it is directly linked to

hygiene practices and limited access to antibiotics and medical care (M. Gewitz, 2015).

Most cases of RHD are only diagnosed after symptoms of heart failure arise and without a clinical history of ARF. Late diagnosis often results in short life expectancy, leading to an estimation of 233,000 deaths per year worldwide. Unlike ARF, advanced cases of RHD are not treatable via secondary prophylaxis, since irreversible damage of the heart tissue is often present (M. Essop, 2014). Surgery is required for these patients, many of which undergo replacement of their native valves. Early detection increases life expectancy significantly. Screening campaigns have shown that most of the early valvar compromise is silent, thus amenable to go undetected on clinical examination alone. Borderline or subclinical RHD cases may not present classical symptoms, but only mild alterations that can only be identified if subject to echocardiography (B. Remenyi, 2012).

Even though echocardiography is one of the most cost effective solutions to screen for heart valve

anomalies, the average socioeconomic context of the affected populations is not favourable to this kind of monitoring RHD patients need. To compensate for the lack of resources, several screening studies have been made in different regions to assess the practicability of some cost reducing measures. In 2015 Lu et al. (J. Lu, 2015) studied the possibility of simplifying the criteria for RHD detection with no substantial losses in sensitivity and specificity. Several studies reported on the feasibility of RHD screenings being done by non-expert health workers such as nurses, after being subject to brief training. Results are favourable and point to the potential use of the technique in low-resources settings. However, erroneous regurgitation jet identification and incorrect measurement are the predominant causes of false positives, as the correct and consistent interpretation of these findings requires experience (M. Ploutz, 2015) (M. Mirabel, 2016) (D. Engelman, 2016). Moreover, the manual annotation of the regurgitation jets is time consuming and is highly operator dependent and subjective (Roelandt, 1986) (R. Castello, 1992). The Automatic detection of regurgitation jets would significantly decrease time and experience dependency of the user. Mitral Regurgitation is visually assessed via parasternal long axis (PLAX) and apical 4 chamber (A4C) views, with colour flow Doppler mode (Figure 1). The pseudo-colour is superimposed on the brightness mode, representing the movement of the blood cells in the heart. The Hue represents the direction of the flow, where the blue and red hues indicate, respectively, that the flow is moving away and towards the transducer. The saturation represents the magnitude of the velocity. Regurgitation jets are often represented in plain blue hues or high saturation colour mosaics (blue, yellow and orange hues) due to turbulence, which may or may not be involved in a blue or red envelope.

In this paper we propose a semi-automatic method for the detection of mitral regurgitation jets candidates, based on HSV space for colour segmentation and localizing active contours for anatomical segmentation. The paper is organized as follows: section 2 describes the materials and methods used for this paper; section 3 presents the proposed method for regurgitation jet detection; section 4 presents the results and discussion for the methods exposed in sections 3; section 5 concludes this paper.

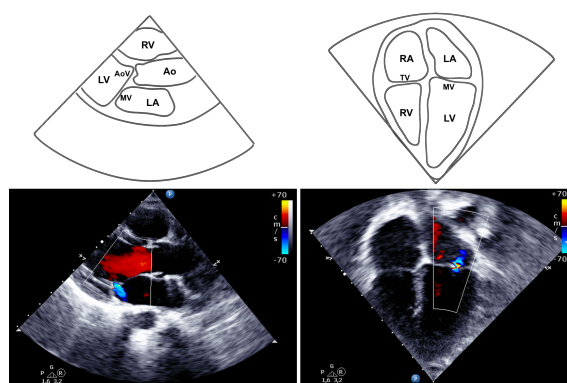


Figure 1: PLAX (left) and A4C (right). Anatomical scheme (top) and colour flow Doppler mode (bottom).

## 2 MATERIALS AND METHODS

### 2.1 Dataset

The dataset used, in this study, consists on 20 sequences of paediatric echocardiography, forming a total of 979 frames, all stored in DICOM format. The sequences were acquired during the Heart Caravan of 2016, a health care provision initiative which took place in the State of Paraíba organized by the non-governmental organization *Círculo do Coração*. Patients were all children, with mean age of 10 years and a standard deviation of 4 years. Half of the patients were female and the other half were male. All the patients presented some degree of mitral regurgitation and 5 of them had a previously established diagnosis of Rheumatic Fever. Eleven of the sequences were acquired with Vivid I, portable echocardiography equipment from GE, with paediatric cardiovascular probe 6S-RS with range of frequency 2.7 to 8 MHz, and image resolution of 422 x 636 pixels. The frames are stored uncompressed, via Explicit VR Little-endian transfer syntax. The other 9 were acquired with CX-50, portable echocardiography equipment from Philips, with the paediatric probe S5-1 with frequency range of 1 to 5 MHz, and image resolution of 600x800 pixels. The frames are compressed in lossless RLE format. Fifteen of the sequences were acquired via parasternal long axis view, and the other 5 via apical four-chamber view.

### 2.2 Manual Annotations

The manual annotations used as ground truth for the results evaluation were drawn by a research associate experienced in echocardiography analysis. Three categories of objects were manually segmented: the

left atrium boundaries, the regurgitation jets and the colour pattern candidates. The colour pattern candidates include detections on the diastole phase, which cannot be related to regurgitation, and detections on the systole phase, which may or may not be related to regurgitation.

### 2.3 Performance Metrics

In the case of mitral regurgitation jets, it is fundamental to have a measure of the portion of jets which are detected. Sensitivity, or true positive rate (1) provide that information:

$$TPR = TP / (TP + FN) \quad (1)$$

On the other hand, it is also important to know if the detection of negatives is achieved. Specificity or true negative rate (2) gives the proportion of well detected negatives for all the real negatives:

$$TNR = TN / (TN + FP) \quad (2)$$

Considering the size of the images and the dimensions of the objects of interest, the majority of the image will be composed of negative samples, very easy to detect (note that a significant part of the image has no information). Therefore, specificity will not be able to measure small variations of jets detection. An alternative to the specificity is the false detection rate (3) which gives the proportion of the false positives in all the detections:

$$FDR = FP / (FP + TP) \quad (3)$$

We will use the same metrics for the segmentation of the left atrium, evaluating the pixels inside or outside of the contour, since the purpose of the segmentation is to define a region of interest and not to get a precise boundary of the chamber.

## 3 REGURGITATION JET DETECTION

The detection of regurgitation jets in colour flow Doppler images requires two phases: colour segmentation and anatomical segmentation. Colour segmentation aims for the detection of the colour patterns of interest, while anatomical segmentation aims to define the region of search for those patterns. The method we propose is represented in Figure 2. Colour segmentation is divided in two phases: pseudo-colour

isolation and colour pattern segmentation. The result is a set of candidates of jet regurgitation. The result of the anatomical segmentation is a set of masks of the left atrium, which confine the search for colour patterns.

Both segmentation phases will be explained throughout this section.

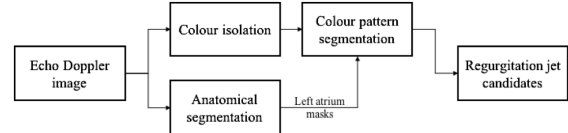


Figure 2: General scheme of the proposed method.

### 3.1 Colour Segmentation

Based on the clinical assumption that mitral regurgitation is always represented by either blue hues (blood cells move away from the ultrasound transducer) or high intensity colour mosaics (yellow and orange hues), we propose a colour-based approach for the segmentation of regurgitation pattern candidates. The pseudo-colour mapping of Doppler flow follows a standard of what is known to be natural and intuitive in terms of the human eye perception. The human perception of colour is often described based on hues and saturation. We choose to work on the HSV (hue-saturation-value) colour space, because it offers the possibility of formulating a mathematical model, based on physicians interpretations of Doppler colour. Hue and Saturation together form the chromaticity, which is the information of colour. Hue describes a pure colour and saturation describes its purity (a measure of the dilution of the colour by white light) (R. Gonzalez, 2008).

#### 3.1.1 Pseudo-colour Isolation

Saturation channel is typically used to isolate regions of interest in the hue channel. Pseudo-colour has inherent high degrees of purity, which translate into high saturation (R. Gonzalez, 2008). Therefore, it is known that the colour information will be present in pixels of high saturation. A mask can be generated by thresholding the saturation channel, to isolate the pseudo-colour from the grayscale tissue background. The area of the mask is taken as a measure of its completeness. A set of thresholds were tested, each one being a percentage between 0% and 100% of the maximum intensity of the Saturation channel, with a step of 10%. The test was made for 15 random samples from the dataset (3 frames from 5 videos) and the results are represented in Figure 3. For thresholds near 0% the area is maximum and for thresholds near

100% the area is minimum. In the middle values it is expected to find a range of thresholds which will lead to similar area values, since the saturation intensities will not vary significantly for the pseudo-colour pixels. Tests confirm the existence of a stabilization plateau, and so, the value in the centre was used as a threshold, which is 50%. An example of the result of colour isolation is represented in Figure 4.

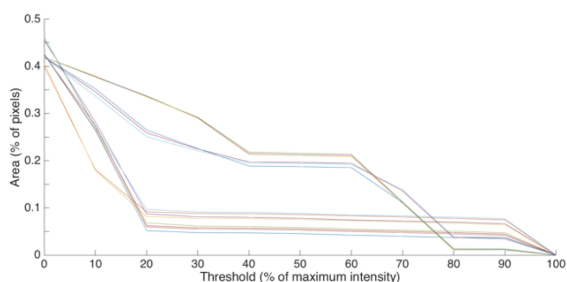


Figure 3: Total mask area for each threshold. Each line represents one frame from 5 randomly selected sequences.

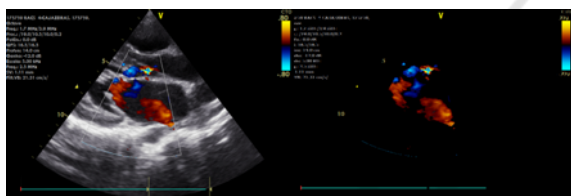


Figure 4: Original PLAX view frame (left) and result from pseudo-colour isolation (right).

### 3.1.2 Colour Pattern Segmentation

As previously stated, pseudo-colour formation in Doppler images relies on the basic convention that reddish and blueish hues represent blood moving towards and away of the probe. When accessing the blood flow through the mitral valve, normal unidirectional flow from the left atrium to the left ventricle should be represented by reddish hues. Other hues are a product of abnormal motion of blood, such as regurgitation (Figure 5) or turbulence.

We propose a colour segmentation based, on the hues, to get candidates of mitral regurgitation. Assuming that we are interested in all hues but reds and dark oranges, a simple threshold of the Hue channel may be sufficient to remove the red component of the pseudo-colour. Yellow and red hues are represented by low magnitudes, whereas blue hues are represented by high magnitudes. The threshold for the red hues removal is roughly defined, during acquisition time, by visual inspection of the colour bar provided by the equipment (Figure 6). The value is set to 10% of the maximum magnitude of the Hue channel.

Since the pseudo-colour in Doppler only repre-

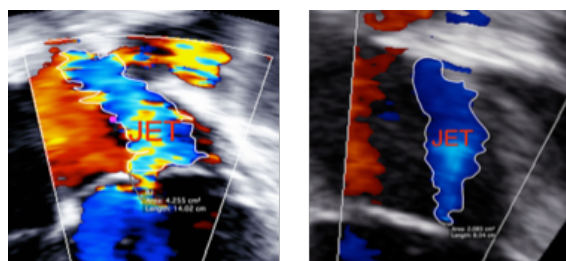


Figure 5: Regurgitation jets in A4C view. Regurgitation is represented in a colour mosaic (left) or in blue hues (right).



Figure 6: Colour-bar from Vivid I, GE and Hue channel magnitude for each colour.

sents one direction of the blood motion, it is expected to have discontinuities in the representation of jets. Physicians will often extrapolate the segmentation of the regurgitation jets to include these regions of predicted regurgitation. The segmentation is refined using morphological methods to cover some of the discontinuities: morphological closing is applied to connect close blobs and flood fill is applied to fill holes.

### 3.2 Anatomical Segmentation

World Health Organization guidelines for the echocardiographic assessment of mitral valve abnormalities indicates the use of the A4C and PLAX windows in the diagnosis criteria extraction. Regurgitation jets should be found within the left atrium region (B. Remenyi, 2012). Both views include other structures of the heart besides the left atrium and the mitral valve complex. When selecting a region of interest on the image for visualization of the colour flow, technicians often include neighbour areas such as part of the left ventricle, the aorta valve or the right atrium. These areas, will also have a Doppler response but, for the assessment of the mitral valve, they are of no use. Because of that we decided to restrict the search zone, so that only the left atrium is analysed.

Automatic segmentation of anatomical structures in ultrasound images is very challenging, due to the low spatiotemporal resolution, inherent acoustic interferences and speckle noise, and lack of intensity and texture differentiation between different tissues (S. Mazaheri, 2015). Active contour models are very popular approaches for medical image segmentation. They usually belong to one of two categories: edge-based or region-based. Edge-based active contour models have good performance segmenting regions

of heterogeneous intensity, but are highly sensitive to noise. Region-based are usually more robust to noise and initialization, but they assume that the intensities of each region to be constant, which makes them not suitable for heterogeneous cases which we often find in ultrasound images. Localizing region-based active contours are proposed with the objective of allying the advantages of both categories while suppressing their drawbacks. Foreground and background can be described in terms of small regions; thus, heterogeneity of the image is not a problem. A disk kernel ( $B$ ) moves along each point of the initial contour, computing exterior and interior energies, as represented in Figure 7. The total energy is given by:

$$E(\phi) = \int_{\Omega_x} \delta\phi(x) \int_{\Omega_y} B(x,y) \cdot F(I(y), \phi(y)) dy dx + \lambda \int_{\Omega_x} \delta\phi(x) \|\Delta\phi(x)\| dx \quad (4)$$

Where  $I$  denotes the input image at the domain  $\Omega$ ,  $\delta\phi(x)$  is the portion of contour centred at  $x$  and  $B$  is the neighbourhood kernel around the point  $(x,y)$ , which is used to define the localizing area. These elements are graphically represented by the red circle ( $B$ ) and the yellow point  $(x,y)$  in Figure 7.  $F$  is the internal energy function. The last term refers to the continuity of the contour line and is scaled by a factor  $\lambda$ .

An energy optimization algorithm will move the point by fitting a model to the region.

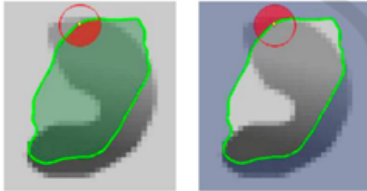


Figure 7: Graphical representation of the localizing active contour method. The red circle is the neighbourhood,  $B$ , of the yellow point  $(x,y)$  (S. Lankton, 2008).

For this work, the internal energy function  $F$  used was the Uniform Model, defined as:

$$F = H(\phi(y))(I(y) - u_x)^2 + (1 - H\phi(y))(I(y) - v_x)^2 \quad (5)$$

Where  $H(\phi(y))$  represents the exterior of the contour in the neighbourhood ( $B$ ) and  $u_x$  represents its mean. While  $(1-H\phi(y))$  represents the interior and  $v_x$  represent its mean (S. Lankton, 2008).

For the left atrium segmentation in 2D+t echocardiographic sequences, we proposed the application of localizing region-based active contours. The Doppler

pseudo-colour that is superimposed in the brightness mode image will interfere with the active contour adjustment. For that reason, we use the mask obtained at the pseudo-colour isolation step, in order to get an estimation of the grayscale brightness mode at the background. The pixels inside the colour mask are passed to the active contours algorithm as low random values (below the average of intensity of the image), to mimic the typical non-tissue speckle affected aspect of the interior of the atrium. This assumption may seem as a possible source of errors for the contour adaptation, specially in cases when the colour mask is significantly large when compared with the atrium. However, practical results suggest this is not a significant drawback for the method. A possible reason for the ability of adaptation of the localizing active contours in these cases is the internal force term, which limits the deformability of the contour, maintaining its shape. The penalizing parameter for the arc-length of the curvature ( $\lambda$ ) must be sufficiently small so it allows deformation of the contour to fit the corners of the atrium, but high enough to prevent leakage. Four values between 0.4 and 1.0 were tested and 0.6 was the one that seemed to keep the best compromise between the requirements.

Minimal user interaction is required for contour initialization: two points, one at the centre of the left atrium and one at the endocardium (inner boundary of the atrium). The initialization mask is a circle centred at the first point with radius equal to the distance between the two points. The stopping condition in this method is the number of iterations. Since the regional mask will move along each point of the contour at each iteration, the process may be computationally heavy. The number of iterations for the first frame was selected empirically after testing multiple values of radius of local region and checking at which number of iterations convergence happened. Frequently there was no further active contour adaptation or improvement around 100 iterations. For the following frames, the contour initialization was given by the previous frame contour result. Assuming that the variation between successive frames is smaller than the variation between the user input mask and the final result of the first frame, the number of iterations for convergence should be smaller. Similar experiment was made for those frames, starting at 100 iterations and reducing gradually. The final iterations number was 50.

Radius of the local region mask is of great relevance for the performance of the algorithm. A study was made by the author (S. Lankton, 2008) to analyse the effect of the radius on the resulting contour. The radius should be chosen considering the scale of

the object to be segmented and its distance to the surrounding. Very small radius makes the internal energy function to approximate on of an edge detector while very large radius make it tend to a global region statistics approach. Once again, a compromise must be made to accommodate both requirements of the local and global features. Intermediate values of radius usually result in similar outcomes, but with different speeds of convergence. Taking the typical dimensions of the left atrium on the echocardiography windows into account, a set of eleven radii were tested from 10 to 20, with a step of 1. Results showed small variation for intermediate values, and a radius of 16 was chosen.

Before being input to the localizing active contours framework, the images are converted into grayscale, a histogram equalization is performed and Gaussian blur is applied for smoothing.

## 4 RESULTS AND DISCUSSION

### 4.1 Colour Pattern Segmentation

The dataset was subject to the colour isolation and pattern segmentation pipeline. The search for patterns was restricted to the regions of the left atrium given by the manual annotations. The results from this process are evaluated against the manual annotations of colour patterns (regurgitation jets and candidates).

The mean values for the performance metrics are: sensitivity of 0.913 and false detection rate of 0.103. Sensitivity shows that more than 91% of the pixels are correctly identified as jets or candidates by the pipeline, which is a satisfactory result. An example can be seen in Figure 9. About 10% of all the detections are false positives. The distribution of the metrics for the 20 cases (Figure 8) show no significant dispersion between quartiles, with only one outlier.

The results suggest the colours of interest are correctly identified.

The anatomical segmentation was applied on the resulting background of the colour isolation of the images. The evaluation is made against the manual annotations of the left atrium. The mean values for the performance metrics are: sensitivity of 0.805 and false detection rate of 0.284.

More than 80% of the pixels belonging to left atria were correctly identified as positives, which means the framework achieved the purpose of defining a rough region of interest. However, the remaining excluded pixels may contain valuable colour information for the regurgitation jet search. 28% of false positives indicate that some parts of the boundary were

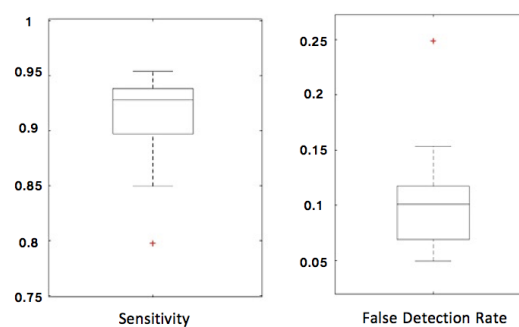


Figure 8: Whiskers plot of sensitivity and false detection rate for colour pattern detection.

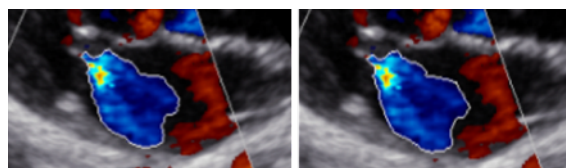


Figure 9: Result of segmentation by the colour pattern segmentation pipeline (left) and manual annotation of the jet (right).

extended to neighbour chambers, which may increase the false detections of regurgitation jets candidates. Examples of both false positives and false negatives can be seen in Figure 11.

The fact that the boundaries are often not represented on the ultrasound image is probably the main source of error for this framework.

The distribution of the results (Figure 10) shows some variability between cases, which may indicate that acquisition conditions affect the performance of the framework.

### 4.2 Regurgitation Jet Detection

The final tests consist in applying the left atrium masks obtained by the localizing active contours framework as the spatial restriction for the colour pattern segmentation, in order to understand the impact caused on the pattern segmentation by the semi-automatic atrium segmentation. The mean values for the performance metrics are: sensitivity of 0.826 and false detection rate of 0.228. The distribution of the results (Figure 12) is similar to the distribution for the left atrium segmentation. It is possible to infer that the faults on the anatomical segmentation decrease the true jet candidates' detection and increase false detections. Both cases can be seen on the examples in Figure 13.

Between the jet candidates, only a small part is identified with confidence as mitral regurgitation. The results for the detection of those candidates is: sensi-

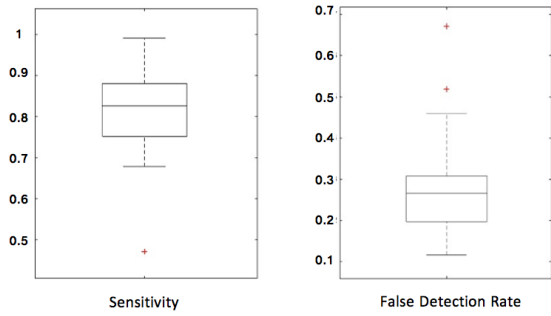


Figure 10: Whiskers plot of sensitivity and false detection rate for left atrium segmentation.

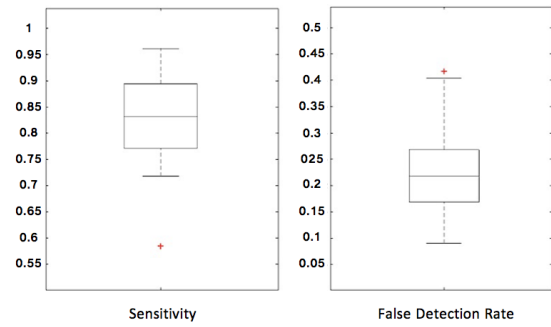


Figure 12: Whiskers plot of sensitivity and false detection rate for the combined pipeline.

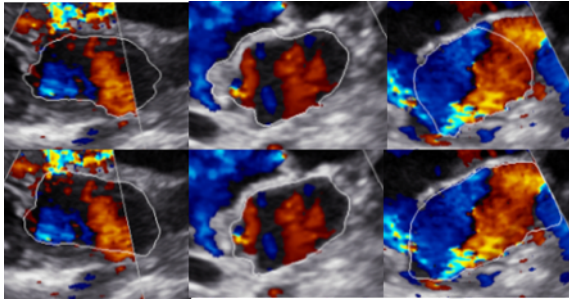


Figure 11: Results of anatomical segmentation (top) and manual annotations (bottom). First column shows a satisfactory result. Second column is an example of overestimation of the atrium area. Third column is an example of underestimation of atrium area.

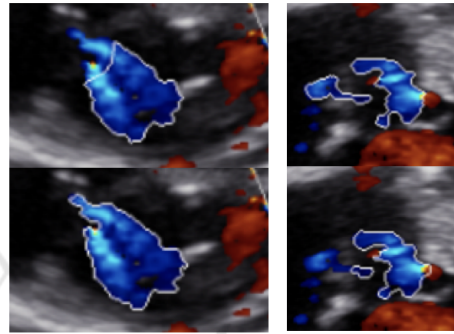


Figure 13: Results of combined pipeline (top) and manual annotations (bottom). Occurrence of false negatives (left) and false positives (right).

tivity of 0.863 and false detection rate of 0.513. The sensitivity increases when compared to the overall detection of patterns. However, the false detection rate is significant, since the images contain a substantial amount of non-regurgitation colour patterns.

Another possibility for false detection suppression, is to confine the search for regurgitation to the systolic phase of the cardiac cycle. The dataset was manually identified as systolic or diastolic and the pipeline was applied only on the systolic group. The results for detection of real jets are: sensitivity of 0.840 and false detection rate of 0.355. As expected, the false detection rate decreases if the diastolic phase is not included, since all the candidates present on that phase are certainly not regurgitation jets.

## 5 CONCLUSION

A new method for the segmentation of the mitral regurgitation jet in sequences of 2D+t Doppler echocardiography is proposed. While the colour patterns of interest are correctly identified as regurgitation candidates, the anatomical spatial restriction step is still far from ideal. Localizing region-based active contours

adapt to the heterogeneity of the left atrium, but do not recover well from discontinuities in the boundary of the atrium. This usually occurs on the part of the boundary formed by the mitral valve, because of the opening of the leaflets. The results confirm that the false positives can be decreased by limiting the search to the systolic phase. The confinement of the search for that part of the cycle may also improve the performance of the localizing region-based active contour, since the leaflets are closed, forming the required boundary. However, the contour initialization for each frame is currently the resulting mask from the previous frame. The division of the sequence into cycles will create the need for a re-initialization strategy for each systole in a sequence

The addition of manual annotations by other subjects may provide more certainty for the classification of the colour pattern candidates, and therefore reduce the false positives. Regarding the colour, it is difficult to determine further characteristics for the distinction of candidates between regurgitation jet and turbulence or other phenomena. Other characteristics such as shape and relative position or orientation of the candidates may be useful to decrease the false detection ratio of the jet detection.

Future developments include the detection of the

cardiac cycle phase and inclusion of characteristics other than colour for jet detection.

## ACKNOWLEDGEMENTS

This article is a result of the project (NORTE-01-0247-FEDER-003507-RHDecho), co-funded by Norte Portugal Regional Operational Programme (NORTE 2020), under the PORTUGAL 2020 Partnership Agreement, through the European Regional Development Fund (ERDF). This work also had the collaboration of the Fundação para a Ciência e Tecnologia (FCT) grant no: PD/BD/105761/2014 and has contributions from the project NanoSTIMA, NORTE-01-0145-FEDER-000016, supported by Norte Portugal Regional Operational Programme (NORTE 2020), through Portugal 2020 and the European Regional Development Fund (ERDF). GE and PHILLIPS for providing the equipment. Health professionals from Círculo do Coração for their volunteer work and data collection. The Health Secretary of Paraíba for their support to the actualization of the Heart Caravan.

## REFERENCES

- B. Remenyi, N. Wilson, A. S. B. F.-J. K. K. J. L. G. M. E. M. M. M. A. M. C. M. J. P. A. S. J. S. J. S. S. V. V. B. G. W. L. Z. J. C. (2012). World heart federation criteria for echocardiographic diagnosis of rheumatic heart disease - an evidence-based guideline. In *Nature Reviews, Cardiology*. I. Macmillan Publishers Limited.
- D. Engelman, J. Kado, B. R. S. C.-J. C. N. W. S. D. A. S. (2016). Screening for rheumatic heart disease: quality and agreement of focused cardiac ultrasound by briefly trained health workers. In *BMC Cardiovascular Disorders*. Springer Nature.
- E. Marijon, D. Celermajer, M. T. S. E.-H. D. J. B. F. X. J. (2009). Rheumatic heart disease screening by echocardiography: The inadequacy of world health organization criteria for optimizing the diagnosis of subclinical disease. In *Circulation*. American Heart Association.
- J. Lu, C. Sable, G. E. C. W.-J. S. T. A. P. L. J. G. A. B. (2015). Handheld echocardiographic screening for rheumatic heart disease by non-experts. In *Heart*. BMJ Publishing and British Cardiology Society.
- M. Essop, F. P. (2014). Contemporary issues in rheumatic fever and chronic rheumatic heart disease. In *Circulation*. American Heart Association.
- M. Gewitz, R. Baltimore, L. T. C. S.-S. S. J. C. B. R. K. T. A. B. L. B. B. M. A. B. N. P. E. K. (2015). Revision of the jones criteria for the diagnosis of acute rheumatic fever in the era of doppler echocardiography. In *Circulation*. American Heart Association.
- M. Mirabel, R. Bacquelin, M. T. C. R.-B. H. P. C. I. F. K. N. J. M. B. N. A. H. B. R. X. J. E. M. (2016). Screening for rheumatic heart disease - evaluation of a focused cardiac ultrasound approach. In *Circ Cardiovascular Imaging*. American Heart Association.
- M. Ploutz, J. Lu, J. S. C. W.-G. E. T. A. P. L. C. S. A. B. (2015). Simplified rheumatic heart disease screening criteria for handheld echocardiography. In *Journal of the American Society of Echocardiography*. American Society of Echocardiography.
- R. Castello, P. Lenzen, A. L. (1992). Quantitation of mitral regurgitation by transesophageal echocardiography with doppler color flow mapping: Correlation with cardiac catheterization. In *Journal of the American College of Cardiology*. American College of Cardiology.
- R. Gonzalez, R. W. (2008). *Digital Image Processing*. Pearson Education, New Jersey, 3rd edition.
- Roelandt, J. (1986). *Color Doppler Flow Imaging and other advances in Doppler echocardiography*. Springer, Netherlands, 1st edition.
- S. Lankton, A. T. (2008). Localizing region- based active contours. In *IEEE Transactions on Image Processing*.
- S. Mazaheri, R. Wirza, P. S. M. D.-F. K. R. T. (2015). Segmentation methods of echocardiography images for left ventricle boundary detection. In *Journal of Computer Science*.